

# The Influence of Grid Rotation in von Neumann and Moore Neighborhoods on Agent Behavior in Pedestrian Simulation

**Machi Zawidzki**

*Department of Architecture  
Massachusetts Institute of Technology  
77 Massachusetts Ave. 7-304G  
Cambridge, MA 02139*

---

Most crowd simulations (CS) in architectural spaces are based on rectangular grids with von Neumann or Moore neighborhoods. A real space, however, is not limited to right angles. This paper focuses on qualitative aspects of CS, namely the agent's behavior. More specifically: whether or not an agent's behavior seems realistic or natural.

---

## 1. Introduction

---

Most crowd simulations (CS) in architectural spaces are based on rectangular grids with von Neumann or Moore neighborhoods. The distance in the former is defined by the von Neumann metric ( $\nu N$ ), and in the latter can be defined by both Manhattan ( $MM$ ) and Euclidean ( $ME$ ) metrics. A real space, however, is not limited to right angles. How does the rotation of the grid influence the simulation? Which type of rectangular discretization of space is the most suitable for non-rectangular layouts? How does the change in grid orientation influence an agent's behavior? Can an agent's strategy compensate for the shortcomings of the neighborhood used? Section 2 briefly discusses the concept of architectural grid. Section 3 presents two simulations based on experiments from literature:

1. A scenario of evacuating 200 agents from a square room with the grid rotated at four angles:  $0^\circ$ ,  $15^\circ$ ,  $30^\circ$ , and  $45^\circ$ .
2. One-directional flow at various pedestrian densities at six angles:  $0^\circ$ ,  $15^\circ$ ,  $18.434^\circ$ ,  $26.565^\circ$ ,  $30^\circ$ , and  $45^\circ$ .

All simulations are performed in  $\nu N$ ,  $MM$ , and  $ME$  grids with three types of agents: Lazy, Conservative, and Perky.

## 2. Space Discretization in Architectural and Urban Design

---

A guideline system is a common aid introduced in various fields of engineering and design, for example, structural and electrical engineer-

ing and architectural, urban, and typographic design. The motivation varies among the fields, however, and usually reflects the design constraints or serves as a compositional aid.

In architecture and city planning, the design space is Euclidean, and there are a number of reasons for using guidelines for creative work: both use guidelines for composition and modularity. In architecture, guidelines also reflect the human scale and structural constraints. In urban design, land partitioning and urban infrastructure are significant guidelines. Throughout history, a number of guideline systems have been developed. Selected examples are briefly described and illustrated in the following subsections.

### ■ 2.1 Regular Grid

A regular grid partitions Euclidean space into identical units of the same area and shape. There are three regular tilings, also called “Platonic”: rectangular (square), triangular, and hexagonal. The symmetry group of regular tilings is transitive on the tiles; in other words, they are homogeneous with respect to vertices, tiles, and edges and are strongly edge homogeneous [1]. This is equivalent to an edge-to-edge tiling by congruent regular polygons. This property has been widely used in architectural practice since antiquity, and the first systematic mathematical treatment was done in the early seventeenth century by Kepler [2]. Figure 1 shows examples of architectural plans based on regular tessellations.

A coarse uniform grid has been introduced in [3] for the architectural functional layout optimization problem. In the case of residential buildings, the functional grid corresponds to the minimum clearance for a corridor, that is, 1 to 1.5 m.

### ■ 2.2 Compound Grid

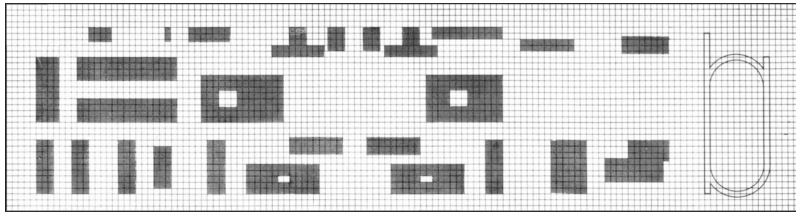
Some designers introduced overlapping or compound grids, allowing different spaces to be discretized differently, as shown in Figure 2.

### ■ 2.3 Hierarchical Systems

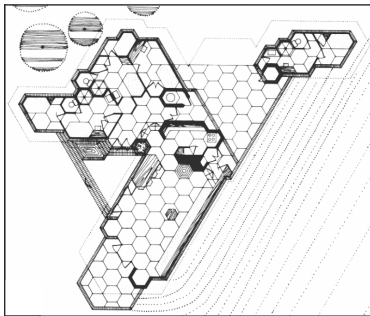
A number of so-called *planned cities* have been laid out using hierarchical systems where the guidelines depend on the scale of the composition, as shown in Figure 2.

### ■ 2.4 Grid for Crowd Simulations

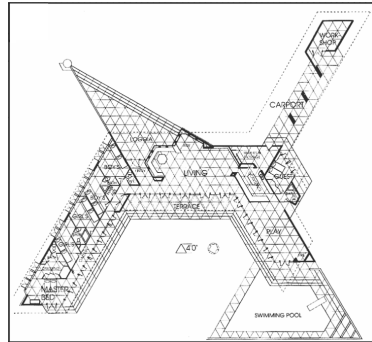
The most common grid for CS is derived from the maximal densities observed in dense crowds, which give the minimal space requirement for one person [4] under the condition that each cell can be occupied by one person at a time. This space requirement can be identified with the cell size. According to [5], a maximal density of 6.25 persons per  $\text{m}^2$  leads to a cell size of  $40 \times 40$  cm.



(a)

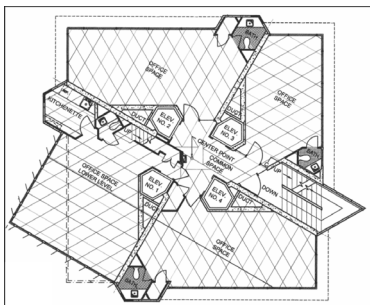


(b)

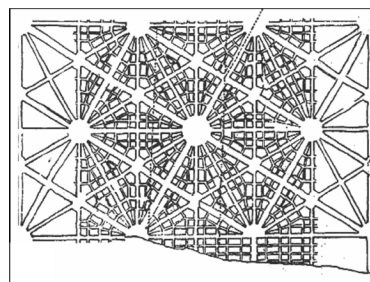


(c)

**Figure 1.** Examples of floor plans in regular tessellations: (a) Mies van der Rohe's plan for the Illinois Institute of Technology campus from 1940 (24' x 24' grid). (b) and (c) Frank Lloyd Wright's residential plans based on hexagonal (Bazett House, 1939) and triangular (Fawcett House, 1955) tessellations, respectively.



(a)



(b)

**Figure 2.** (a) A typical floor of the Price Tower by Frank Lloyd Wright (completed in 1956). (b) The original plan for Detroit by Augustus B. Woodward (1805).

However, space discretization for CS is usually done without much consideration of an architectural grid system. Therefore, the CS grid and its orientation might not integrate well with the geometry of the walls in the plan. As a result, the agents in very simple models might not move naturally in a given space, as demonstrated in Section 3.

### 3. The Simulation in Crowd-Z

The simulations have been performed in Crowd-Z (CZ)—the user-friendly platform for simple CS in architectural plans introduced in [7]. CZ is very intuitive, and is intended not only for designers and specialists, but also for users such as students, security staff, and others. For illustrative examples of CZ, see [8].

In the following simulations, the basic setup of CZ has been used, that is, an agent-based model (ABM) with a distance field (DF) [9]. The movement of agents is determined by the local neighborhood defined by DF and can be expressed by the following rules:

- If all of the neighboring cells are occupied, either by other agents or walls—wait.
- Check the values of DF in the available neighboring cells and act according to the “perkiness.”

The perkiness describes the willingness of an agent to move. In this model, there are three possibilities listed in Table 1.

Perkiness	Description
Lazy	Only moves to a neighboring cell if its value in DF is lower than the current one.
Conservative	Will also move to an equipotent DF cell.
Perky	May move to any allowable neighboring cell.

**Table 1.** Three standard agent strategies in CZ.

The simulations have been performed in three types of DFs based on von Neumann ( $\nu N$ ), Moore with Manhattan ( $MM$ ), and Moore with Euclidean ( $ME$ ) metrics, as illustrated in Figure 3. In order to avoid conflicts among agents choosing the same location for the next step, random shuffled update is used [10]. “Setup” refers to the combination of the neighborhood type, the metric, and agent perkiness. Error rate ( $eR$ ) is a parameter introducing randomness to agent movement. For each agent at each step,  $eR$  is the probability of making a random decision among possible choices. For  $eR = 0$ , there is no additional randomness, whereas for  $eR = 1$ , agents perform a random walk. In all experiments,  $eR$  is set to 0, which means that agent movement is extremely efficient.

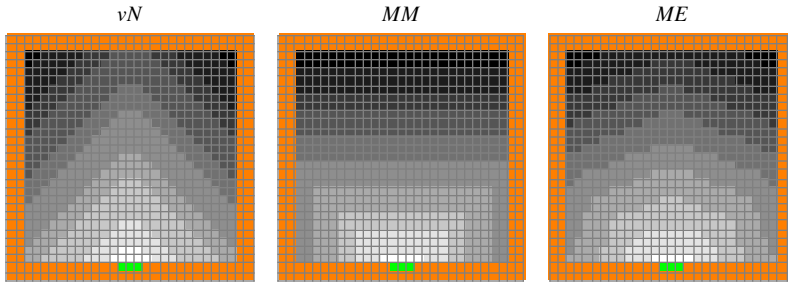


**Figure 3.** The floor plan for the first experiment. The walls and three exits are indicated in orange and green, respectively. The farther from the exits, the darker the cells. For improved visibility, the images have been posterized.

Usually CS focus on quantitative results such as egress time, agent flow, and so on. This paper, however, studies simple qualitative characteristics of a simulation, namely whether the agents move naturally. To illustrate this intuitively, a so-called “heat map” (HM) has been used. A HM records the frequency of agent visits to each cell, which is visualized by the color saturation (Experiment 1) or hue (Experiment 2) of cells.

### ■ 3.1 Experiment 1: Evacuation from a Square Room

The first experiment is based on the simulation of evacuation described in [6], where 200 agents are to leave a  $25 \times 25$ -cell room through a 3-cell exit. In addition to the original setup, the grid has been rotated by three angles:  $15^\circ$ ,  $30^\circ$ , and  $45^\circ$  in relation to the layout, as shown in Figure 4.

Since the number of “walkable” cells must be the same (625) in each grid position, some manual corrections have been applied.

Figure 5 collects the HMs illustrating agent behavior in all setups of this experiment.

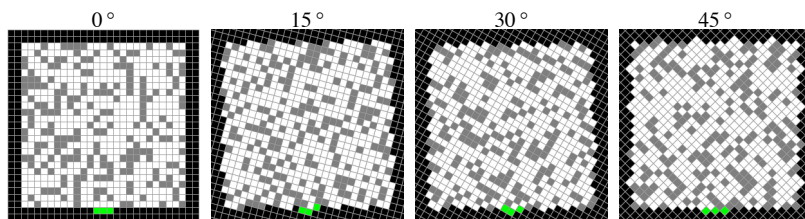


**Figure 4.** From the left: the layout with the original grid and three grids at  $15^\circ$ ,  $30^\circ$ , and  $45^\circ$  angles, respectively. Two hundred randomly distributed agents are shown in gray. The exit cells are shown in green.

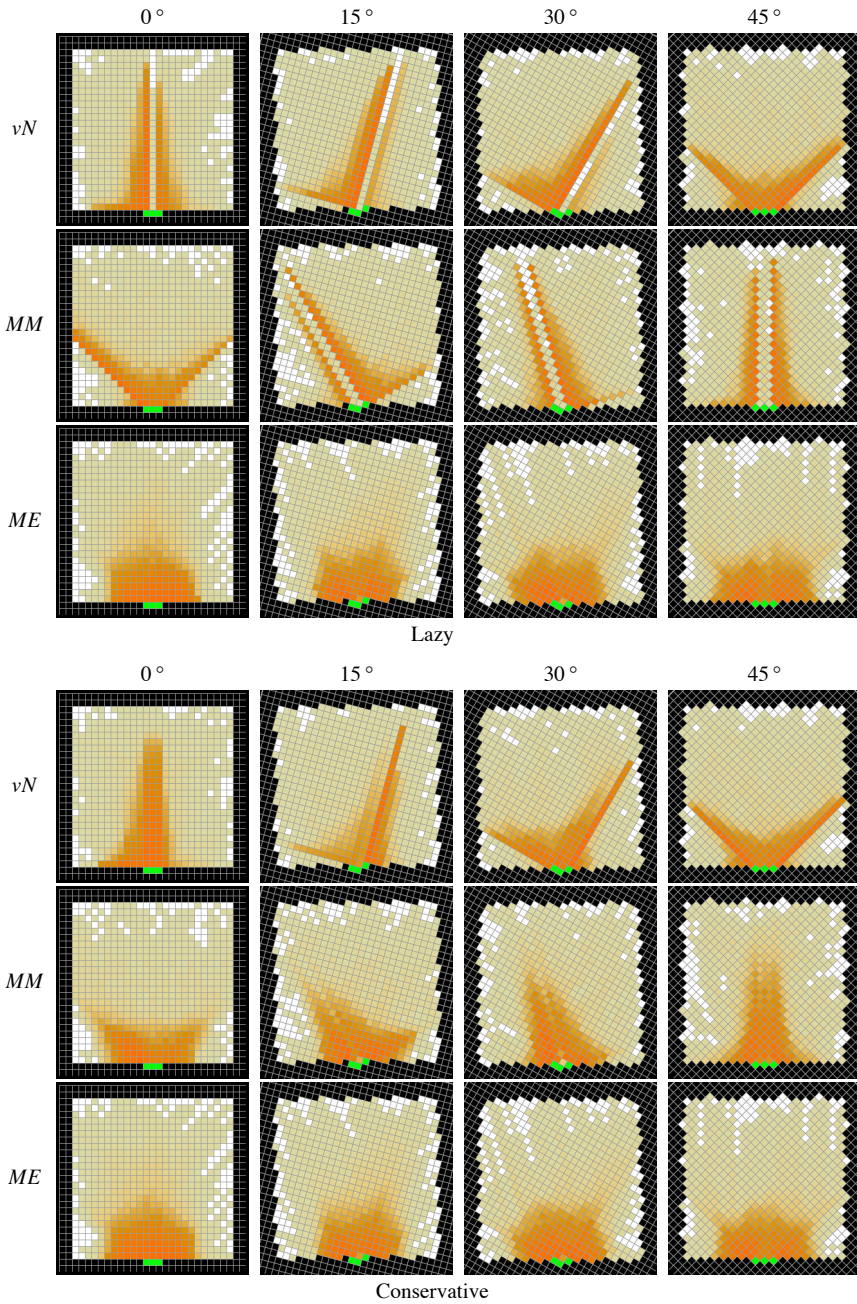
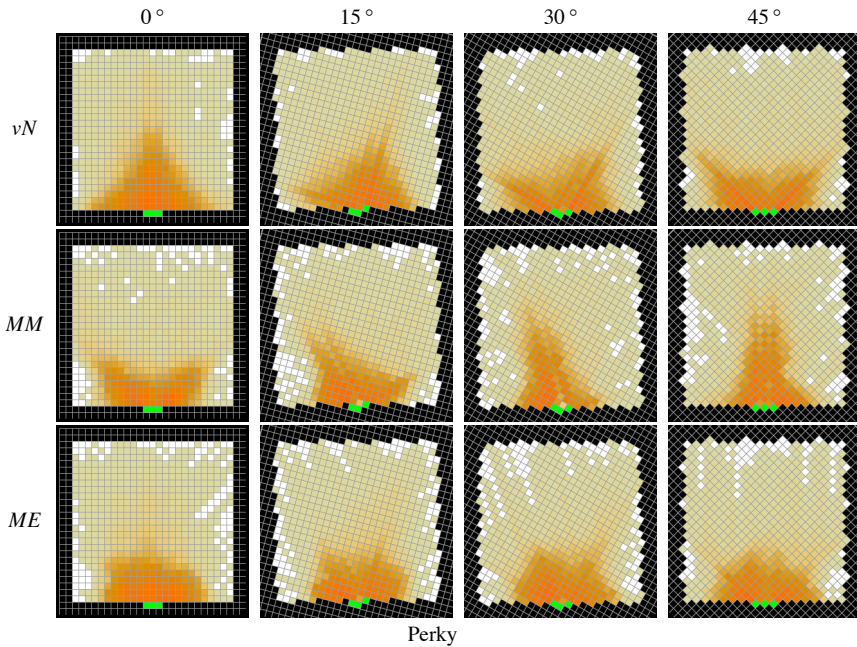


Figure 5. (continues).



**Figure 5.** HMs for all types of agents. The exits are indicated in green. *ME* is the least affected by the grid rotation. *Perky* agents move the most naturally.

As Figure 5 indicates, the behavior of agents is highly influenced by the model used. This is also reflected in quantitative data. Figure 6 compares the evacuation time of all setups, averaged from 10 trials.

As Figure 6 indicates, *vN* is the most sensitive to the grid rotations, regardless of agent perkiness. *MM* with Conservative and *Perky* agents and *ME* regardless of agent perkiness are relatively consistent.

### ■ 3.2 Experiment 2: One-Directional Flow

The simulation of one-directional crowd flow along four types of inclined pathways at 0°, 18.434°, 26.565°, and 45° has been analyzed in [12]. The modeling of agent behavior used there is more sophisticated than here. It included implementation of “personal space,” variable velocity, and other factors. The quantitative data, namely density-velocity and density-flow rates, showed rather good agreement with the Japanese Public Guideline for Evacuation. Certain discrepancies observed in the flow rates among different inclinations were attributed to “the difference between the directional vectors of pedestrians and the direction of pathways model.” The inclination angles considered in [12], however, are derived from the square grid, as shown in

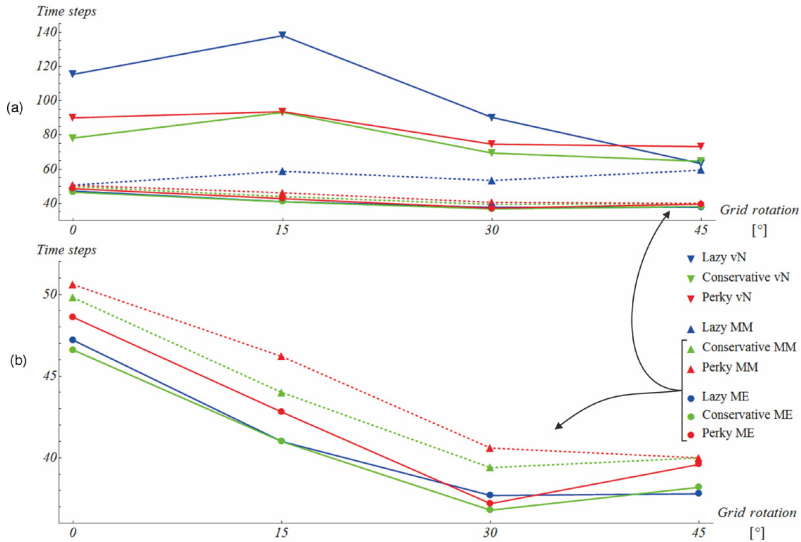


**Figure 6.** (a) The average evacuation time steps for all agent types, DFs, and grid rotations. (b) Five relatively consistent setups in more detail.

Figure 7. Such a procedure generates the following sequence of angles:  $45^\circ$ ,  $26.565^\circ\dots$ ,  $18.434^\circ\dots$ ,  $14.036^\circ\dots$ ,  $11.309^\circ\dots$ ,  $9.462^\circ\dots$ ,  $8.1301^\circ\dots$ ,  $7.125^\circ\dots$ ,  $6.3401^\circ\dots$ ,  $5.7105^\circ\dots$ ,  $5.19443^\circ\dots$ , and so on. Other than  $45^\circ$ , all such angles are irrational numbers. Most importantly, there are only four angles greater than  $15^\circ$ , and the rest of them are very acute. Thus the applicability of this method for architectural layouts in general is very limited. Usually architecture uses arbitrary or rational angles, such as  $15^\circ$ ,  $18^\circ$  (for pentagon),  $45/2^\circ$ ,  $30^\circ$ ,  $270/7^\circ$  (for heptagon),  $45^\circ$ , and so on. Therefore, in the simulations presented in this subsection, two additional angles have been included:  $15^\circ$  and  $30^\circ$ .

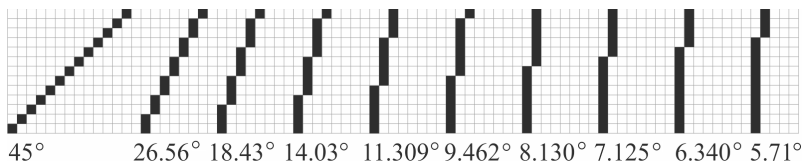


**Figure 7.** Azimuthal inclination angles derived from the square grid.

Figure 8 collects HMs that illustrate agent behavior in all setups in this experiment. The crowd density ( $\rho$ ) is 3.125 agents per  $m^2$ , that is, 50% of the maximum. As Figure 8 indicates, in this very simple



model, the agents move naturally only in the simplest cases, that is, at  $0^\circ$  and  $45^\circ$  angles. At other inclinations, a certain asymmetry is evident. Although *ME* is the least unnatural, even there agents tend to move along one of the walls. For *ME* and  $\nu N$ , this tendency is stronger for smaller angles. Conversely, for *MM* it is stronger for wider angles. Interestingly, there is a certain antisymmetry between HMs for  $\nu N$  and *MM*. Figure 9 shows density-flow rate diagrams for all types of agents, metrics, and path inclination angles for crowd densities up to 6.25 agents per  $m^2$  (maximum). As Figure 9 indicates, in all but one setup the density-flow rate reflects the natural transition from *free walking state*, when the flow rate grows (ideally, proportionally) with increasing crowd density  $\rho$ , to the *crowd flow state*, when flow rate stabilizes. The only exception that clearly stands out is *MM* with Lazy agents at  $30^\circ$ . Interestingly, although according to Figure 8 Conservative and Perky agents in *MM* do not move in a particularly natural way, these setups show the highest consistency in density-flow rates.

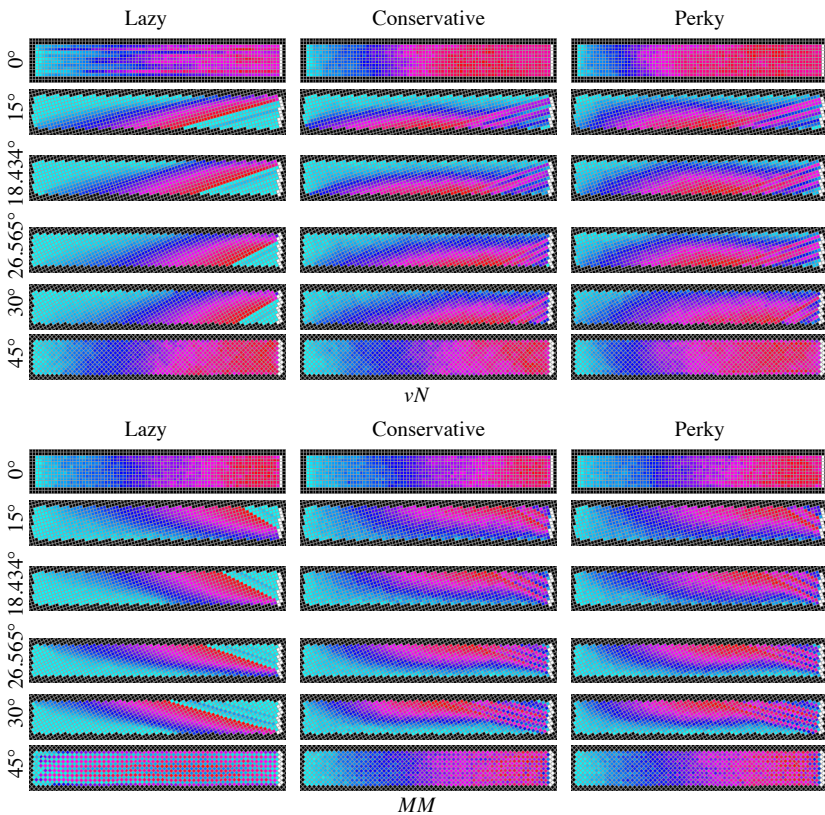
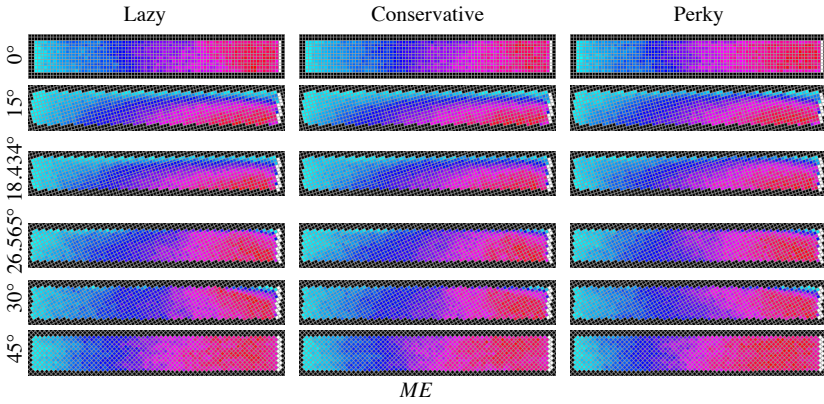
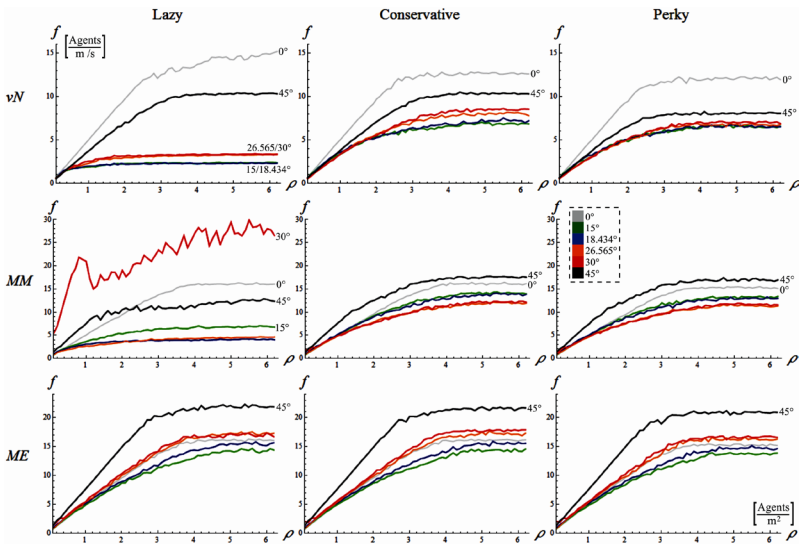


Figure 8. (continues).



**Figure 8.** HMs for all types of agents, metrics, and inclinations. The exits are indicated in white. Hue is the color function. None of the setups cause agents to move naturally at all inclinations. However, *ME* is the most natural, especially with Perky agents.



**Figure 9.** Density-flow rate diagrams for all types of agents, metrics, and path inclination angles.

Figure 9 also indicates that density-flow rate is higher than the actual number of pedestrians. However, as demonstrated in [7], it can be reduced by increasing the value of  $eR$ .

In most setups, density-flow rates for angles derived from a square grid,  $18.434^\circ$  and  $26.565^\circ$ , are very similar to rational angles,  $15^\circ$  and  $30^\circ$ . Most importantly, HMs do not indicate substantial differences between the aforementioned angles. This suggests that the findings presented in [12] would hold for any arbitrary angle.

#### 4. Conclusions

---

The concerns about oversimplified models that result in unrealistic behavior of agents have been expressed a number of times in literature. In particular, the shortcomings of pedestrian modeling based on the von Neumann metric have been stressed in the past. Several adjustments to the model have been proposed. For example [11] introduced the wall potential and contraction effect at a wide exit to improve the modeled behavior near corners and bottlenecks. However, most of these methods have not been validated for rotated grids.

As Figures 5 and 8 indicate, depending on the combination of simulation parameters (“setup”), the rotation of a grid may cause the agents to behave more or less unnaturally. It is particularly evident in the case of the simplest neighborhood type—von Neumann (*vN*). Thus, in general, it is not recommended for crowd simulations (CS) in architectural spaces. Not surprisingly, the Euclidean metric in a Moore neighborhood (*ME*) is the most appropriate, as it also models the real space in the most exact way.

On the other hand, the type of agent behavior also has a substantial influence on crowd movement and can alleviate the deficiency of an oversimplified metric. In general, Perky agents move relatively the most naturally.

#### Acknowledgments

---

This work was completed as part of the Singapore University of Technology & Design and Massachusetts Institute of Technology Postdoctoral Fellows Program (SUTD-MIT PDP). The research is titled: *Effective computational methods for grid and raster-based modeling of practical problems in architectural and urban design layouts*.

#### References

---

- [1] D. Chavey, “Tilings by Regular Polygons—II: A Catalog of Tilings,” *Computers & Mathematics with Applications*, 17(1–3), 1989 pp. 147–165. doi:10.1016/0898-1221(89)90156-9.

- [2] J. Kepler, *The Harmony of the World* (E. J. Aiton, A. M. Duncan, and J. V. Field, trans.), Philadelphia: American Philosophical Society, 1997.
- [3] M. Zawidzki, K. Tateyama, and I. Nishikawa, "The Constraints Satisfaction Problem Approach in the Design of an Architectural Functional Layout," *Engineering Optimization*, **43**(9), 2011 pp. 943–966. doi:10.1080/0305215X.2010.527005.
- [4] A. Schadschneider and A. Seyfried, "Empirical Results for Pedestrian Dynamics and Their Implications for Modeling," *Networks and Heterogeneous Media*, **6**(3), 2011 pp. 545–560. doi:10.3934/nhm.2011.6.545.
- [5] U. Weidmann, "Transporttechnik der Fussgänger Transporttechnische Eigenschaften des Fussgängerverkehrs," Literatúrauswertung (in German), Schriftenreihe des IVT 90, ETH Zurich, 1993.
- [6] C. Rogsch, A. Schadschneider, and A. Seyfried, "Simulation of Human Movement by Cellular Automata Models Using Different Update Schemes," in *Proceedings of 4th International Symposium: Human Behaviour in Fire 2009*, Robinson College, Cambridge, UK, London: Interscience Communications Ltd., 2009 pp. 543–548.
- [7] M. Zawidzki, M. Chraïbi, and K. Nishinari, "Crowd-Z: The User-Friendly Framework for Crowd Simulation on an Architectural Floor Plan," *Pattern Recognition Letters*, **44**, 2014 pp. 88–97. doi:10.1016/j.patrec.2013.10.025.
- [8] M. Zawidzki. "Crowd-Z." (Sep 22, 2014) <http://zawidzki.com/Crowd-Z>.
- [9] T. Kretz, S. Hengst, and P. Vortisch, "Pedestrian Flow at Bottlenecks: Validation and Calibration of VISSIM's Social Force Model of Pedestrian Traffic and Its Empirical Foundations," in *3rd International Symposium on Transport Simulation (IST 2008)* (M. Sarvi, ed.), Queensland, Australia: Monash University, 2008.
- [10] N. Rajewsky, L. Santen, A. Schadschneider, and M. Schreckenberg, "The Asymmetric Exclusion Process: Comparison of Update Procedures," *Journal of Statistical Physics*, **92**(1–2), 1998 pp. 151–194. doi:10.1023/A:1023047703307.
- [11] K. Nishinari, A. Kirchner, A. Namazi, and A. Schadschneider, "Extended Floor Field CA Model for Evacuation Dynamics," *IEICE Transactions on Information and Systems*, **E87-D**(3), 2004 pp. 726–732.
- [12] S. Koyama, N. Shinozaki, and S. Morishita, "Pedestrian Flow Modeling Using Cellular Automata Based on the Japanese Public Guideline and Application to Evacuation Simulation," *Journal of Cellular Automata*, **8**(5–6), 2013 pp. 361–382.